Published in "Journal of Biochemical Chemistry 281(29): 19830-19839, 2006"
which should be cited to refer to this work.

ETHANOLAMINEPHOSPHATE SIDE CHAIN ADDED TO GPI ANCHOR BY MCD4P IS REQUIRED FOR CERAMIDE REMODELING AND FORWARD TRANSPORT OF GPI PROTEINS FROM ER TO GOLGI

Yonghua Zhu,* Christine Vionnet and Andreas Conzelmann

Department of Medicine/Biochemistry, University of Fribourg, Switzerland

Running title: ethanolaminephosphate on yeast GPI anchors

Corresponding author e-mail: andreas.conzelmann@unifr.ch
Dr. A. Conzelmann, Division of Biochemistry, Chemin du Musée 5, CH-1700 Fribourg, Switzerland.
Tel. ++41 26 300 8630. Fax ++41 26 300 9735.
* Current address : Institute of life science and Biotechnology, Hunan University, 410082 Changsha city, P.R.China

Glycosylphosphatidylinositol (GPI) anchors of mammals as well as yeast contain ethanolaminephosphate side chains on the α1-4 and the α1-6 linked mannoses of the anchor core structure (protein-CO-NH-(CH_2)-PO_4-6Manα1-2Manα1-6Manα1-4GlcNH_2-inositol-PO_4-lipid). In yeast, the ethanolaminephosphate on the α1-4 linked mannose is added during the biosynthesis of the GPI lipid by Mcd4p. *MCD4* is essential because Gpi10p, the mannosyltransferase adding the subsequent α1-2-linked mannose, requires substrates with an ethanolaminephosphate on the α1-4 linked mannose. The Gpi10p ortholog of *T. brucei* has no such requirement. Here we show that the overexpression of this ortholog rescues *mcd4Δ* cells. Phenotypic analysis of the rescued *mcd4Δ* cells leads to the conclusion that the ethanolaminephosphate on the α1-4 linked mannose, beyond being an essential determinant for Gpi10p, is necessary for an efficient recognition of GPI lipids and GPI proteins by the GPI transamidase, for the efficient transport of GPI anchored proteins from ER to Golgi and for the physiological incorporation of ceramides into GPI anchors by lipid remodeling. Furthermore, *mcd4Δ* cells have a marked defect in axial bud site selection while this process is normal in *gpi7Δ* and *gpi1*. This suggests that also axial bud site selection specifically depends on the presence of the ethanolaminephosphate on the α1-4 linked mannose.

Introduction

The carbohydrate structure linking the C-terminal end of glycosylphosphatidylinositol (GPI) anchored proteins to the lipid moiety is identical in GPI anchors from all organisms analyzed so far, but the GPI anchors from various species differ widely with regard to the side chains attached to this core structure as well as the lipid moieties of the anchor (1, 2). This report concerns the ethanolaminephosphate (EtN-P) side chain, which is often present on mannose 1 of the core structure (Man1 in Fig. 1). Indeed, an EtN-P is found on Man1 of GPI lipids and GPI proteins in mammals, *Saccharomyces cerevisiae* and *Torpedo californica*, and possibly *Candida albicans*, but is not found in other organisms such as *Trypanosoma brucei*, *Leishmania major* or *Plasmodium falciparum* (3-7). The EtN-P-transferase transferring EtN-P to Man1 is encoded by *MCD4* in yeast and its ortholog PIG-N in mammals (Fig. 1)(8, 9). Phosphatidylethanolamine (PE) serves as a donor of the EtN-P group (10). Yeast also possesses two *MCD4* homologs, *GPI7* and *GPI13*, which are involved in the transfer of EtN-P to Man2 and Man3, respectively (Fig. 1). *MCD4* is essential and can be inhibited by YW3548 (6). Addition of this inhibitor or the depletion of Mcd4p arrest the growth of yeast cells and lead to the accumulation of the abnormal GPI lipid M2* (Manα1-6Manα1-4GlcNH_2-inositol-PO_4-lipid), indicating a problem with the addition of Man3 (Fig. 1)(6,

7, 9, 11). This suggested that Gpi10p strongly prefers substrates carrying an EtN-P substituent on Man1. Indeed, overexpression of Mcd4p can improve the growth of yeast cells in the presence of low concentrations of YW3548, while overexpression of Gpi10p is comparatively inefficient (9, 11). While these data indicate that Mcd4p helps Gpi10p by providing an optimal substrate, they can't rule out the possibility that *MCD4* would influence the function of Gpi10p in another way, e.g. by regulating PE levels in the ER or by channeling substrate into Gpi10p or stabilizing Gpi10p.

There indeed is a genetic link between *MCD4* and PE biosynthesis: The *mcd4-P301L* and *mcd4-174* alleles render cells temperature sensitive (ts) when combined with *psd1Δ*, the later eliminating the phosphatidylserine decarboxylase, by which the bulk of PE is made. The *mcd4-P301L* mutation was claimed to not affect GPI biosynthesis. Temperature sensitivity of *mcd4 psd1*Δ mutants could be reverted by the addition of ethanolamine or choline or ethanolamine and sorbitol to the media (12). Temperature sensitivity of another *mcd4* allele named *fsr2-1* is suppressed by overexpression of *PSD1*, *PSD2* or *ECM33* (13).

Mutations in *MCD4* also show several other, quite specific phenotypes, which may not be related to its effect on GPI biosynthesis. Mutants in *MCD4* (mitotic check point dependent 4) were found to suffer from delayed bud emergence and an inability to polarize secretion to the bud tip or septum, thus becoming dependent on a checkpoint delaying mitosis until a bud is formed (14). Buds of *mcd4-174* are small, misshapen and contain many aberrant membrane structures (8). Certain *mcd4* mutants also activate one branch of the hyperosmotic response pathway and are more resistant to high concentrations of Cu^{2+} than wt cells (15).

GPI lipids and GPI anchors of *Trypanosoma brucei* do not contain any EtN-P side chains and thus, their presence certainly will not be required by the *T. brucei GPI10* ortholog (3, 16). In order to test the relationship between *MCD4* and *GPI10* and explore the various functions of *MCD4* more closely, we tested if it was possible to overcome the lethality of the *mcd4Δ* deletion by introducing *T. brucei* Gpi10p into *mcd4Δ* cells. The results show that in this way it is possible to create a cell, in which all functions of Mcd4p are lost while some GPI biosynthesis is preserved.

Experimental Procedures

Strains, growth conditions and materials

Saccharomyces cerevisiae strains used were ***MCD4/mcd4***Δ, *MAT***a** / α *his3Δ1/his3Δ1 leu2Δ0/leu2Δ0 lys2Δ0/LYS2 MET17/met17Δ0 ura3Δ0/ura3Δ0 YKL165c::kanMX4/YKL165c* (EUROSCARF); **T1**, *MAT***a** *his3Δ1 leu2Δ0 ura3Δ0* p425-*TbGPI10*; **T2**, *MAT*α *his3Δ1 leu2Δ0 ura3Δ0 met17Δ0* p425-*TbGPI10*; **T3**, *MAT***a** *his3Δ1 leu2Δ0 ura3Δ0 mcd4::kanMX4* p425-*TbGPI10*; **T4**, *MAT*α *his3Δ1 leu2Δ0 ura3Δ0 met17*Δ*0 mcd4::kanMX4* p425-*TbGPI10*; ***MCD4*** (17A-H42), *MAT***a** *trp1-289 ura3-52 leu2* and ***mcd4^{ts}*** (521-17A-H42), *MAT***a** *trp1-289 ura3-52 leu2 ssu21* (17); MKY3, *MAT*α *trp1 lys2 ura3 leu2 his3 psd1Δ-1::TRP1 mcd4-P301L etn^{-} ^{ts}* (ethanolamine dependent at 37°C) and MKY13, *MAT***a** *arg4 ura3 his3 trp1 leu2 psd1Δ-1::TRP1 mcd4-174* (12); BY4742, *MAT*α *his3Δ1 leu2Δ0 lys2Δ0 ura3Δ0* (EUROSCARF); ***yap3Δ***, *YLR120c::kanMX4* in BY4742 (EUROSCARF); ***gpi8*** (164-1C) *MAT*α *his4 leu2*; ***gpi8 sec18*** (FBY91), *gpi8-1 sec18-1^{ts} leu2-3,112* (7); ***gpi1Δ*** *MAT***a** *ura3-52 his3::hisG gpi1::URA3* pRS425-*CCW12HA*; ***gpi1***, *MAT*α *ura3-52 lys2 gpi1* (isolated as *cwh4* by Frans Klis); ***gpi7Δ***, *YJL062w::kanMX4* in BY4742 (EUROSCARF); ***elo3Δ***, *YLR372W::kanMX4* in BY4742 (EUROSCARF). Cells were grown on rich medium (YPD) or minimal media (SD) (18) containing 2% glucose (D) as a carbon source and uracil (U), adenine (A) and amino acids (aa) as required at 30°C. Methionine was added at 10 mg/L (38 μM), so that the *MET17* promoter was almost fully active. Oligonucleotide synthesis and DNA sequencing services were provided by MICROSYNTH, Balgach, Switzerland. Verification of deletions was done by PCR as shown if Fig. 2C using the following primers: F1 = 5'-ATGTGGAACAAAACCAGAAGGAC-3', F2 = 5'-CACACACGGTGGATCCTGTACAC-3', R1 = 5'-GCTCGATGGAAGATTGCG-3', R2

= 5'-AGCAATCATAGCAACATGACC-3', R3 = 5'-CAAGGAGGGTATTCTGGGC-3', F4 = 5'-CGCGGATCCATGCCGTGGTGGTTGATTTC-3', R4 = 5'-CGGAATTCCGTCACTTCGTCACCTTGACCC.

Construction of yeast vectors

The *T. brucei GPI10* behind the *MET17* promoter on a multicopy plasmid (p425-*TbGPI10, LEU2*) was the kind gift of Howard Riezman and Taroh Kinoshita (16). The promoter and open reading frame of *MCD4* was amplified by PCR and inserted into YEp352 to yield pBF639 (*URA3*). Sequence verification showed a point mutation I387T (at DNA level: T1160C), but the plasmid was able to fully complement *mcd4*Δ mutants.

Cell extraction and Western blotting

Proteins were extracted by incubating cells for 5 min in NaOH and boiling at 95°C in reducing sample buffer (19). Alternatively, cells were broken by glass beads in TEPI buffer (100 mM Tris-HCl, pH 7.5, 10 mM EDTA, 30 μg/ml of each, leupeptine, antipain, and pepstatin, 2 mM PMSF) at 4°C, and the lysate was directly solubilized in octyl-β-glucoside (50 mM) at 4°C for 30 min. After solubilization, the extracts were centrifuged at 16'000 g for 30 min at 4°C and the supernatant was precipitated with trichloroacetic acid (TCA) and boiled in reducing sample buffer as above. In other experiments, cells were broken by glass beads in TEPI buffer, the lysate was directly treated with DNAse (Fluka 31136) for 45 min at room temperature, then the lysate was solubilized with Triton X-114 (1%) at 4°C for 30 min. After solubilization, insoluble material was removed by centrifugation at 16'000 g x 5 min at 4°C. The supernatants were separated into detergent (D) and aqueous (A) phases at 37°C followed by mild centrifugation. The detergent (D) and aqueous (A) fractions were then precipitated with TCA. For treatment with phosphatidylinositol-specific phospholipase C (PI-PLC), the detergent phase was diluted and treated with PI-PLC from *B. cereus* (Sigma P 5542 or Funakoshi Pharm BR-05) using 1 U /ml at 37°C for 2 h with occasional shaking. After a further phase separation the detergent and aqueous phases were precipitated with TCA and processed as above. As primary antibodies we used purified mouse anti-CPY (MOLECULAR PROBES), rabbit anti-Yap3p (a kind gift from Dr. Niahm Cawley) and rabbit anti-Gas1p, made in the lab. As secondary antibodies for blots we used fluorescent goat anti-mouse IgG conjugated to AlexaFuor680 or goat anti-rabbit IgG conjugated to IRDye800 and fluorescence was measured with the Odyssey Imaging system (LI-COR). Alternatively, blots were revealed with goat anti-rabbit IgG conjugated to peroxidase and using ECL technology (Amersham Biosciences).

Analysis of GPIs

GPI lipids were analyzed by metabolic labeling of yeast cells with [^{3}H]*myo*-inositol and labeling of yeast microsomes with UDP-[^{3}H]GlcNAc as described before (7). Head groups of GPI lipids were analyzed with HF using the protocol originally developed by Mike Ferguson (7) and remodeling of lipids on GPI anchors was analyzed by liberating anchor lipids from anchor peptides using HNO_2 as described (20).

Microscopy

To stain cells with calcofluor white, cells were kept in continuous exponential growth for >10 generations, one A_{600} unit of cells was washed with water, stained in calcofluor white (1 mg/ml) for 10 to 20 min at room temperature, washed again and observed under the microscope.

Results

T. brucei Gpi10p can rescue viability of *mcd4Δ* cells

The multicopy vector p425-*TbGPI10* harboring *TbGPI10* behind the *MET17* promoter was introduced into a *mcd4Δ*::*KanMX*/*MCD4* heterozygous diploid strain. The transformed diploid was sporulated and tetrads were dissected. Very few complete tetrads were obtained. Fig. 2A shows a complete tetrad, in which geneticin resistance and methionine auxotrophy segregated 2:2 (Fig. 2B), suggesting that spores T3 and T4 were *mcd4Δ*::*Kan*MX. PCR analysis

confirmed the *mcd4Δ*::*Kan*MX genotype and the presence of the p425-*TbGPI10* plasmid in T3 and T4 (Fig. 2C). The *mcd4::KanMX* strains grew rather slowly. The generation times at 30°C in liquid SDaaUA medium of T1, T2, T3, T4, were 2.48, 2.39, 5.25 and 6.03 hours, respectively. The corresponding generation times in YPDUA were 1.53, 1.61, 7.38 and 6.15 hours, respectively (not shown). The *MET17* promoter driving *TbGPI10* expression is 3 - 5 times more active in the absence of methionine (21). Omission of methionine from minimal medium to achieve a higher expression of *TbGPI10* did not enhance the growth rate of *MET17 mcd4Δ*::*Kan*MX cells (not shown). On plates the *mcd4Δ/TbGPI10* cells grew at almost the same rate at 24 °C, 30°C and 37°C but they were inositol dependent at 37°C (Fig. 2D). The growth rate of *mcd4Δ/TbGPI10* cells on plates at 37°C was also increased by 1M sorbitol and slightly improved by ethanolamine, and the greatest effect on colony size was observed when all these ingredients were combined (Fig. 2D). Sorbitol has been reported to rescue certain *mcd4* mutants (12, 22). However, the p425-*TbGPI10* plasmid did not allow various temperature sensitive *mcd4* strains (*ssu21, mcd4-174, mcd4-P301L)* to grow at restrictive temperature (37°C)(not shown), neither in the presence nor absence of ethanolamine. This may suggest a possible dominant negative effect of these mutant alleles.

The *mcd4Δ/TbGPI10* cells accumulate an abnormal GPI lipid

To investigate the structure of the GPI lipids made by *mcd4Δ/TbGPI10* strains**,** we labeled intact cells with [^{3}H]inositol and analyzed the lipid extracts by TLC and fluorography. In wild type (wt) cells, no GPI lipids can be detected in this way, but certain mutants deficient in GPI biosynthesis or GPI addition to proteins were shown to accumulate significant amounts of labeled biosynthetic intermediates (23). As seen in Fig. 3A, there is an abnormal lipid accumulating in T3 and T4 *mcd4Δ/TbGPI10* strains, which is absent from the T1 and T2 *MCD4* strains (lanes 5, 6 vs. 2, 3). This lipid was named M4* as it has about the same mobility as M4/2, which is one of the several abnormal GPI lipids accumulating in GPI transamidase mutants such as *gpi8 sec18* (Fig. 3A, lane 7). While CP2 contains an EtN-P group on Man1, Man2 and Man3 (Fig. 1), *gpi7Δ* mutants accumulate M4/1 (Fig. 3A, lane 4), which lacks the EtN-P on Man2, while preserving the EtN-P's on Man1 and Man3 (23). The head group of M4* could be released by mild deacylation followed by PI-PLC treatment and, as shown in Fig. 3B, treatment of the liberated head group with HF and acetic anhydride yielded a Man_4-GlcNAc-Inositol fragment. This partial analysis of lipid M4* is compatible with the idea that M4* is a CP2 lacking EtN-P on Man1, thus being the most mature GPI lipid we theoretically can expect in *mcd4Δ/TbGPI10* cells (Fig. 1). When the *mcd4-P301L* (MKY3) or *mcd4-174* (MKY13) strains were labeled with [^{3}H]inositol at 37°C, neither M4* nor any other late GPI intermediate were detectable as reported before (12) (not shown). Moreover, this was also true when these cells expressed *TbGPI10* and independent of the presence or absence of ethanolamine in the labeling medium (not shown). This again points to a possible dominant negtive effect of these *mcd4* alleles.

To further investigate the GPI biosynthesis pathway we prepared microsomes and incubated them with UDP-[^{3}H]GlcNAc. As shown in Fig. 3C, the mature GPI lipid CP2 (Fig. 1) was not detectable in *mcd4Δ/TbGPI10* strains T3 and T4 (lanes 3, 4). However, *mcd4Δ/TbGPI10* strains showed an abnormal accumulation of lipid 4c (Fig. 3C, lanes 3, 4; open triangles), which also accumulates in a temperature sensitive *mcd4* mutant at 37°C (Fig. 3C, lane 8), and which has previously been characterized as Man-Man-GlcN-(acyl→)PI (7). The *mcd4Δ/TbGPI10* strains do not accumulate lipid 031b (Man-Man-Man-(EtN-P→)Man-GlcN-(acyl→)PI), an intermediate containing 3 mannoses and accumulating in Gpi13p-depleted strains (24), and they make no M4/1 (Man-(EtN-P→)Man-Man-(EtN-P→)Man-GlcN-(acyl→)PI), typical of *gpi7Δ* strains (Fig. 3C, lane 7). The presence of the abnormal lipid 4c in *mcd4Δ/TbGPI10* indicated that TbGpi10p was rather inactive under the *in vitro* conditions used here. This is confirmed by the fact that the *gpi10Δ/TbGPI10* strain accumulates M2* (Fig. 3C, lane 6; open circle), a lipid previously characterized as Man-(EtN-P→)Man-GlcN-(acyl→)PI (25). (Interestingly,

traces of a lipid migrating to the position of M4* are visible in T1 and T3, but not T2 and T4, and the same lipid is also present in *gpi10Δ/TbGPI10* (Fig. 3C, lanes 1, 3, 6; asterisk). This potential M4* correlate was only observed in microsomes from *MET17*, not in *met17Δ* strains and the difference may be related to different expression levels of TbGpi10p.)

Incorporation of [^{3}H]inositol into proteins is a measure of GPI protein biosynthesis and was found to be markedly reduced in *mcd4Δ/TbGPI10* (Fig. 3D). Most affected were the mature proteins, which, after glycan elongation in the Golgi, appeared as a high molecular weight smear. Their absence suggests that *mcd4Δ/TbGPI10* cells may have difficulty in transporting proteins to the Golgi (see below).

Immature GPI proteins accumulate in the *mcd4Δ/TbGPI10*

To see if GPI lipids are transferred onto GPI proteins at a normal rate, we analyzed the GPI protein Gas1p, whose ER form migrates at 105 kDa and whose mature form, produced by elongation of N- and O-glycans upon arrival in the Golgi, migrates at 125 kDa by SDS-PAGE. As long as a GPI anchor is not added to Gas1p in the ER, the protein is not packaged into COPII vesicles and not transported to the Golgi so that it accumulates as an immature 105 kDa form (26, 27). Indeed, any significant reduction of GPI lipid biosynthesis leads to an increase of the immature 105 kDa form of Gas1p (28). A previous report shows that the ER-to-Golgi transport of Gas1p is blocked in the *mcd4-174* mutant at restrictive temperature while transport of other proteins such as CPY is unaffected (8). As can be seen in Fig. 4A, in *mcd4Δ/TbGPI10* cells the mature 125 kDa Gas1p was less abundant than in corresponding wt cells while the immature 105 kDa form was present in normal or increased amounts (see below). Moreover, the mutant cells did not accumulate the typical ER and Golgi proforms of CPY named p1 and p2, respectively, and the mature vacuolar form of CPY was present in normal amounts. The p1 proform of CPY was however drastically increased in the *sec18* secretion mutant incubated for 1h at 37°C (not shown). This suggested that the defect of *mcd4Δ/TbGPI10* only affects GPI proteins. The *mcd4Δ/TbGPI10* cells release Gas1p into the medium (Fig. 4B), and this phenomenon is only partially explained by cell lysis, as relatively less immature Gas1p is found in the medium than in the cells. Release of mature GPI proteins could be shown more clearly for Yap3p (see below).

To assay the rate of transport of immature Gas1p to the Golgi, the amount of immature Gas1p was also determined after incubation of cells with cycloheximide (CHX). As shown in Fig. 5A, the relative amounts of immature Gas1p (sum of aqueous and detergent phases) is reduced five fold during a 20 min incubation in the presence of CHX in T1 wt cells (from 10 down to 2 %), while in the mutant T3 only a small fraction of immature Gas1p disappears (from 49% down to 40%). Thus, immature Gas1p seems to be transported only very slowly out of the ER in the *mcd4Δ/TbGPI10* mutant. As mentioned above, GPI-proteins accumulate in the ER when they fail to be anchored but accumulation of GPI proteins in the ER is also observed in other instances: the transport of GPI proteins to the Golgi also fails if COPI, or sphingolipid biosynthesis, or the Emp24p complex, or yet other factors are deficient (for review see (29)). To see if the immature Gas1p accumulating in *mcd4Δ/TbGPI10* is anchored or not, we partitioned Gas1p before and after PI-PLC treatment in the detergent Triton X-114 (30). Figure 5B indicates that the percentage of immature Gas1p that partitions into the aqueous phase due to the action of PI-PLC treatment is higher in *mcd4Δ/TbGPI10* than in wt cells (62 vs. 50%). (It should be noted that it is difficult to shift the total of GPI proteins into the aqueous phase by this technique. In Fig. 5B, even for the mature, GPI-anchored form, only a fraction could be shifted, namely 37% in wt and 42% in *mcd4Δ/TbGPI10*). Importantly, as the percentages of Gas1p shifted by PI-PLC from detergent to aqueous phase are higher for immature than for mature Gas1p, there is no indication that immature, non-anchored Gas1p, would be accumulating, neither in wt nor in *mcd4Δ/TbGPI10* mutant cells. There are reports showing that during Triton X-114 solubilization at 4°C, part of GPI-anchored proteins are recovered in the detergent-insoluble pellet. The efficiency of

solubilization in our experiment was evaluated by probing equivalent samples of the detergent-insoluble pellet and the detergent extract (Fig. 5C). Although Triton X-114 only solubilized 62 % and 80% of Gas1p in wt and mutant cells, respectively, immature Gas1p was solubilized nearly quantitatively in both strains. Thus, the results obtained in Figs. 5A and 5B are representative for the total of immature Gas1p. Pulse chase analysis confirmed the severe transport block of Gas1p (Fig. 5D).

To generalize the data obtained with Gas1p we also investigated the fate of another GPI protein, Yap3p (Yps1p). Yap3p, a 570 amino acids long protein containing 10 potential N-glycosylation sites was described as a 68 kDa GPI-anchored protein (31), but in other reports using the same antibodies, the immature forms of this protein ran as 80 kDa (32) or as 80 and 100 kDa proteins (33) or as bands at 85 and 115 kDa (34), whereas mature forms ran as a broad smears around 150-200 kDa. As can be seen in Fig. 6A, the *mcd4Δ/TbGPI10* mutant (T4) contained much less of the mature (140 - 240 kDa) Yap3p form than the wt (T2) strain or the *gpi1Δ* mutant, but it accumulated an immature 75-100 kDa ER form. Further analysis showed that, similar to Gas1p, Yap3p was secreted from cells into the medium (Fig. 6B). Significantly, the secreted Yap3p consisted mainly of mature Yap3p whereas in the cell lysate, the mature form of Yap3p was relatively minor. Thus, it seems that the appearance of Yap3p in the culture medium of *mcd4Δ/TbGPI10* cells is not due to cell lysis but rather the secretion of a mature Yap3p form. Secretion of GPI proteins has previously been noted in *gpi* mutants, e.g. in *gpi3* (35). GPI anchoring of Yap3p was tested using PI-PLC and TX-114 partitioning as done for Gas1p in Fig. 5B. About 60 % of the mature Yap3p could be shifted from detergent to aqueous phase by PI-PLC in the wt as well as the mutant (Fig. 6C). Again, the *mcd4Δ/TbGPI10* mutant T3 showed a strong accumulation of 75 and 95 kDa ER forms and only 7 % of this material could be shifted from the detergent to the aqueous phase by PI-PLC, as the bulk of it partitioned to the aqueous phase even after mock treatment. (It should be noted that in Fig. 6C the amount of immature Yap3p is severely underestimated, because PI-PLC treatment was done with the Triton X-114 detergent phase and the bulk of the immature Yap3p had already been lost into the aqueous phase of the initial phase separation done to produce this detergent phase that was then treated with PI-PLC). Low amounts of the same 75 and 95 kDa ER forms were visible in the detergent phase of wt cells and were efficiently shifted from the detergent to the aqueous phase by PI-PLC (Fig. 6C, not quantitated). The region <65 kDa contains non-specific bands. During CHX treatment, the 75-95 kDa ER forms vanished in wt cells, but not in *mcd4*Δ/*TbGPI10* cells (not shown). A control analogous to Fig. 5C showed that Triton X-114 had quantitatively extracted Yap3p form T3 while a small percentage of mature Yap3p of T1 remained in the pellet (not shown). We interpret these results as to mean that Yap3p, quite in contrast to Gas1p, fails to be anchored efficiently in *mcd4Δ/TbGPI10* and accumulates in an unanchored form in the ER. This interpretation is based on the observation that non-anchored Gas1p partitions into the aqueous phase during Triton X-114 phase separation (30, 36) and the assumption that the same may hold for unanchored Yap3p. To summarize, in *mcd4Δ/TbGPI10* cells, Yap3p accumulates in the ER, a small amount is anchored and remains cellular, a larger part travels through the Golgi and ends up in the medium. It is presently unclear if that latter material is first anchored but secreted because its structurally abnormal anchor is hydrolyzed at the cell surface, or if this material is transported through the Golgi in an unanchored form.

The *mcd4Δ/TbGPI10* cells do not introduce ceramides into their GPI anchors in the ER

The mature GPI proteins contain a different lipid moiety than the primary GPI lipid, which is attached to them after they have entered the ER. This primary GPI lipid probably contains the C16 and C18 fatty acids typically found in phosphatidylinositol in yeast (37). Most mature GPI proteins of yeast contain a ceramide moiety, whereas a minor fraction contains a modified diacylglycerol containing C26:0 in *sn2* (34, 37, 38). Thus, all mature GPI proteins of yeast endowed with lipid moieties containing C26 or hydroxylated C26 fatty

acids, and the mature lipid moieties are introduced by a remodeling step that replaces the primary lipid moiety. As shown in Fig. 7, lanes 5 - 7, T1 and T2 *MCD4/TbGPI10* cells make a normal set of anchor lipids, namely pG1, a C26:0-containing PI species migrating slightly faster than the abundant PI present in the lipid extract of wt cells (lane 4), and IPC/B and IPC/C, containing PHS-C26:0 and PHS-C26:0-OH, respectively. In contrast, T3 and T4 *mcd4Δ/TbGPI10* cells make only pG1, but no IPCs (Fig. 7, lanes 8, 9). Their ceramide biosynthesis however must be normal since they make a normal set of sphingolipids (Fig. 7, lanes 1 - 3), although in lower than normal quantities. This probably is a consquence of the slower growth rate and a concomitant slowing of the transfer of [^{3}H]inositol-phosphate from PI to ceramide.

Cell wall biogenesis and bud site selection are defective in *mcd4Δ/TbGPI10* cells

Many mutations in the GPI biosynthesis pathway cause cell wall fragility, for which the cell tries to compensate by inducing chitin biosynthesis, and cells therefore become hypersensitive to calcofluor white, a chitin binding toxic compound. *mcd4* mutants being affected in GPI biosynthesis not unexpectedly display osmotic sensitivity and lysis in hypotonic media, increased sensitivity to calcofluor white, SDS, zymolyase, caffeine and staurosporine, an inhibitor of Pkc1p (17, 39). As shown in Figs. 8A and 8B, *mcd4Δ/TbGPI10* cells were hypersensitive to calcofluor white, caffeine, and neomycin and also were unable to survive a sudden heat shock (Fig. 8C). In spite of these several signs of cell wall fragility, *mcd4Δ/TbGPI10* cells didn't display any hypersensitivity to SDS and were not hypersensitive to staurosporine (not shown), suggesting that the cells are osmotically competent. Thus, certain symptoms of cell wall fragility are present in *mcd4Δ/TbGPI10* cells but others, typically present in *mcd4* mutants, are absent. The *mcd4Δ/TbGPI10* cells also were Cu^{2+} hypersensitive (Fig. 8B), while certain *mcd4* alleles had been shown to be copper resistant (15).

Compared to wt cells, the *mcd4Δ/TbGPI10* cells are unusually large and grow in small clumps of round cells (not shown). A similar phenotype of abnormally large and round cells, growing in small clumps because of a cell separation defect, has been described in a *mcd4* mutant and has been attributed to its inability to polarize its secretion apparatus (14, 17). Microscopic inspection of haploid *mcd4Δ/TbGPI10* cells after calcofluor white staining indicated that cells have only slightly more chitin in their cell walls than wt cells but that they have a defect in axial bud site selection. Many cells, in stead of the normal axial, showed a bipolar, or unipolar or random bud site selection pattern (Fig. 9A). The same bud site selection defect was equally seen when cells were grown in minimal medium but in this medium they also had more chitin all over their cell walls (not shown). As a positive control we used *elo3Δ* cells, which do not show the normal axial pattern but exhibit a mix of bipolar, unipolar and random bud site selection patterns (Fig. 9B) (40). Transfection of *mcd4Δ/TbGPI10* with a plasmid harboring the wt *MCD4* gene abolished the bud site selection defect, since buds faithfully emerged next to the previous bud emergence site (Fig. 9A).

The same bud selection defect was also found in the *mcd4^{ts}* strain grown at semi-permissive temperature (32° and 34°C)(Fig. 9B). These mutant cells additionally exhibited a deregulated bud emergence generating multibudded cells (Fig. 9B), a phenomenon which was only very occasionally observed in *mcd4Δ/TbGPI10*. The *gpi7Δ* and *gpi1* mutants (Fig. 1), lacking an EtN-P on Man2 or being unable to make GPI anchors at elevated temperatures (41) did not exhibit any bud site selection defect (Fig. 9B), although *gpi1* mutants generate multibudded cells (41). These findings suggest that bud site selection is not just dependent on the synthesis of sufficient amounts of GPI proteins but specifically depends on the EtN-P on Man1.

Discussion

Our report shows that the essentiality of *MCD4* in yeast can be suppressed by the presence of *T. brucei GPI10*, an enzyme that allows the

completion of GPI lipids beyond the stage of the Man_2-GlcN-acyl-PI intermediate that has been shown to accumulate in *mcd4*^{ts} mutants (7). This reconfirms the previously postulated importance of the EtN-P side chain on Man1 for yeast Gpi10p and the correctness of the idea that *MCD4* is required for addition of Man3 because it allows the biosynthesis of the correct substrate for Gpi10p (9, 11). The resulting *mcd4*Δ/*TbGPI10* yeast strain grows more slowly than wt and shows various abnormalities in the biosynthesis and transport of GPI proteins but it would appear that neither the enzymes required to transform the Man_3-GlcN-acyl-PI into a mature GPI nor the transamidase have an absolute requirement for a EtN-P on Man1 (Fig. 1). In contrast to yeast, the human *MCD4* ortholog PIG-N is not required for the survival of tumor cell lines *in vitro* (9). *In vivo* metabolic labeling with [^{3}H]-mannose of PIG-N knock out (KO) cells shows that the GPI biosynthesis stops at H7' (mammalian equivalent of M4*) instead of H8 (mammalian equivalent of CP2), but quantitatively there is not more H7' in PIG-N KO cells than there is H8 in wt cells, while transamidase mutants such as the hGAA1 KO cells accumulate massive amounts of H8 and of earlier GPI intermediates (9). Although these KO tumor cell lines may be genetically unstable and therefore not truly comparable amongst each other, one naively may interpret the above findings to mean that the human transamidase uses GPI lipids lacking EtN-P on Man1 quite efficiently, or else, that the transamidase is absolutely not rate limiting in the mammalian system. In contrast, the accumulation of M4* in *mcd4*Δ/*TbGPI10* cells (Fig. 3A) suggests that yeast transamidase does not work efficiently with GPI lipids lacking EtN-P on Man1 or else, that the GPI transamidase of *mcd4*Δ/*TbGPI10* cells is blocked by anchored GPI proteins, which accumulate because they are not efficiently transported to the Golgi. These two possibilities are not mutually exclusive. The latter idea is however less likely, since no accumulation of CP2 can be observed in *sec18* at 37°C, which accumulate GPI anchored proteins in the ER due to a secretion block (42). Thus, we believe that the transamidase is working more slowly in *mcd4*Δ/*TbGPI10* because M4* is not its optimal substrate. This is also supported by the finding that the amount of [^{3}H]inositol-labeled proteins is severely reduced (Fig. 3D), and that a certain GPI proteins accumulate as unanchored ER forms. Intriguingly, this was only observed with Yap3p, while Gas1p was efficiently anchored. How can we explain this different fate of Gas1p and Yap3p?

The quality of the GPI attachment signal and hence the probability that a protein will be GPI anchored can be calculated using the algorithms elaborated by Birgit Eisenhaber and coworkers displayed at http://mendel.imp.univie.ac.at/home/Birgit.Eisenhaber/index.html. The predictor for fungi gives GPI anchoring probability scores between 5 and 20 for most of the ascertained GPI proteins of yeast, a score of 13.7 for Gas1p, but a score of only 0.65 for Yap3p. Nevertheless, data in Fig. 6C indicate that in wt cells (T1) at least 59% of Yap3p are GPI anchored confirming an earlier report by others (31). The available microsomal assays for the GPI transamidase allowed to establish that the Gpi8p protease attacks the ω residue, thereby allowing the C-terminal anchor attachment signal to leave and forming a covalent acyl intermediate, which in turn is attacked by the GPI lipid to release the enzyme. It is conceivable that the binding of GPI lipid and protein substrate to the enzyme is cooperative and that low score GPI proteins such as Yap3p are more dependent on this cooperative effect for efficient anchoring than high score proteins such as Gas1p. Thus, we speculate that in *mcd4*Δ/*TbGPI10* cells the lack of appropriate GPI lipids may lead to a deficiency of GPI anchoring, which specifically affects low score proteins.

In yeast, the reduced surface expression of GPI proteins in *mcd4*Δ/*TbGPI10* can be traced to several reasons, depending on the protein: Gas1p seems to be inefficiently transported and, in addition, to be lost into the medium, Yap3p also is lost from the surface and additionally is not anchored efficiently. The analysis of the lipid anchor of Gas1p only identified fatty acids but no ceramide (38); thus, the lack of ceramide remodeling cannot directly be responsible for the failure of *mcd4*Δ/*TbGPI10* cells to transport Gas1p from the ER to the Golgi. One possiblity is that EtN-P on Man1 is required for the interaction of Gas1p with the cargo receptor Emp24p, which was shown to physically interact with Gas1p (43).

The complete absence of ceramide anchors in *mcd4Δ/TbGPI10* cells suggests that, similar to *GPI10*, the hypothetical ceramide remodelase requires the presence of EtN-P on Man1. Alternatively, it also may be that, beyond being the EtN-P transferase, *MCD4* also acts as a ceramide remodelase, capable of exchanging diacylglycerol for ceramide. Indeed EtN-P transferase and remodelase reactions are similar in that both represent transterification reactions involving phosphodiester linkages. The possibility that Mcd4p acts as ceramide remodelase is also supported by the fact that the deletion of *GPI7* (Fig. 1) leads to a specific defect of ceramide remodeling in the Golgi (23). This possibility is presently further investigated.

MCD4 mutants were isolated in many different contexts and found to be deficient in many apparently unrelated biological functions. As the *mcd4Δ/TbGPI10* cells not only lack EtN-P on Man1 of the GPI anchored proteins, but also exhibit a severe reduction of many GPI proteins on their surface, we tried to compare their phenotype with the ones of the few other viable *gpi* mutants hoping to identify some characteristics that may give us a hint about a more specific function of the EtN-P on Man1 and the introduction of ceramide into the GPI anchors in the ER. Such a specific function was recently suggested for the EtN-P on Man2, added by Gpi7p: Lack of EtN-P on Man2 leads to a missorting of the daughter cell specific, GPI-anchored endoglucanase Egt2p (44). We started to investigate this phenotype in *mcd4Δ/TbGPI10*, but abandoned because >90% of the HA-tagged Egt2p was secreted by both wt (T1) and *mcd4Δ/TbGPI10* (T3) in the form of a 65 kDa fragment (reducing SDS-PAGE) rather than the expected >100 kDa form (not shown).

We find a distinct bud site selection defect in all *mcd4Δ/TbGPI10* cells. While many genes are known to affect the bipolar bud site selection in diploid cells, much fewer genes are known to affect the normal axial budding pattern of haploid cells, and the two classes of genes are largely non-overlapping (45). Of the few genes related to GPI protein expression, the deletion of *GAS1, CCW12, BST1* and *GPI7* affect only bipolar bud site selection in diploids, but were found to be without any effect on budding in haploid cells (40). Obviously, if GPI anchoring were required for bud site selection, this may easily have been overlooked, as most deletion mutants in the GPI anchor biosynthesis pathway of yeast are lethal. Here we report on a bud site selection defect of *mcd4Δ/TbGPI10*. This finding suggests that some GPI anchored protein(s) may be important for bud site selection in haploids. At the same time our data show that haploid *gpi7Δ* and *gpi1* and *bst1Δ* mutants don't exhibit a similar defect (Fig. 9B)(40). Further work is necessary to firmly establish and understand the specific role of the EtN-P side chain on Man1 in axial bud site selection.

References

1. Ferguson, M. A. J., Kinoshita, T. and Hart, G. W. (in press) in Essential Glycobiology, *2nd edition* (Varki, A., Bertozzi, C., Cummings, R., Etzler, M., Esko, J., Freeze, H., Hart, G. and Stanley, P., eds.)

2. Kinoshita, T. and Inoue, N. (2000) *Curr Opin Chem Biol* **4**, 632-638

3. Ferguson, M. A., Homans, S. W., Dwek, R. A. and Rademacher, T. W. (1988) *Science* **239**, 753-759

4. McConville, M. J., Collidge, T. A., Ferguson, M. A. and Schneider, P. (1993) *J Biol Chem* **268**, 15595-15604

5. Homans, S. W., Ferguson, M. A., Dwek, R. A., Rademacher, T. W., Anand, R. and Williams, A. F. (1988) *Nature* **333**, 269-272

6. Sutterlin, C., Horvath, A., Gerold, P., Schwarz, R. T., Wang, Y., Dreyfuss, M. and Riezman, H. (1997) *EMBO J* **16**, 6374-6383

7. Imhof, I., Flury, I., Vionnet, C., Roubaty, C., Egger, D. and Conzelmann, A. (2004) *J Biol Chem* **279**, 19614-19627

8. Gaynor, E. C., Mondesert, G., Grimme, S. J., Reed, S. I., Orlean, P. and Emr, S. D. (1999) *Mol Biol Cell* **10**, 627-648

9. Hong, Y., Maeda, Y., Watanabe, R., Ohishi, K., Mishkind, M., Riezman, H. and Kinoshita, T. (1999) *J Biol Chem* **274**, 35099-35106

10. Imhof, I., Canivenc-Gansel, E., Meyer, U. and Conzelmann, A. (2000) *Glycobiology* **10**, 1271-1275

11. Sutterlin, C., Escribano, M. V., Gerold, P., Maeda, Y., Mazon, M. J., Kinoshita, T., Schwarz, R. T. and Riezman, H. (1998) *Biochem J* **332**, 153-159

12. Storey, M. K., Wu, W. I. and Voelker, D. R. (2001) *Biochim Biophys Acta* **1532**, 234-247

13. Toh-e, A. and Oguchi, T. (2002) *Genes Genet Syst* **77**, 309-322

14. Mondesert, G., Clarke, D. J. and Reed, S. I. (1997) *Genetics* **147**, 421-434

15. Toh-e, A. and Oguchi, T. (2001) *Genes Genet Syst* **76**, 393-410

16. Nagamune, K., Nozaki, T., Maeda, Y., Ohishi, K., Fukuma, T., Hara, T., Schwarz, R. T., Sutterlin, C., Brun, R., Riezman, H. and Kinoshita, T. (2000) *Proc Natl Acad Sci U S A* **97**, 10336-10341

17. Packeiser, A. N., Urakov, V. N., Polyakova, Y. A., Shimanova, N. I., Shcherbukhin, V. D., Smirnov, V. N. and Ter-Avanesyan, M. D. (1999) *Yeast* **15**, 1485-1501

18. Sherman, F. (2002) *Methods Enzymol* **350**, 3-41

19. Kushnirov, V. V. (2000) *Yeast* **16**, 857-860

20. Guillas, I., Pfefferli, M. and Conzelmann, A. (2000) *Methods Enzymol* **312**, 506-515

21. Mumberg, D., Muller, R. and Funk, M. (1994) *Nucleic Acids Res* **22**, 5767-5768

22. Maneesri, J., Azuma, M., Sakai, Y., Igarashi, K., Matsumoto, T., Fukuda, H., Kondo, A. and Ooshima, H. (2005) *J Biosci Bioeng* **99**, 354-360

23. Benachour, A., Sipos, G., Flury, I., Reggiori, F., Canivenc-Gansel, E., Vionnet, C., Conzelmann, A. and Benghezal, M. (1999) *J Biol Chem* **274**, 15251-15261

24. Flury, I., Benachour, A. and Conzelmann, A. (2000) *J Biol Chem* **275**, 24458-24465

25. Canivenc-Gansel, E., Imhof, I., Reggiori, F., Burda, P., Conzelmann, A. and Benachour, A. (1998) *Glycobiology* **8**, 761-770

26. Nuoffer, C., Horvath, A. and Riezman, H. (1993) *J Biol Chem* **268**, 10558-10563

27. Doering, T. L. and Schekman, R. (1996) *EMBO J* **15**, 182-191

28. Benghezal, M., Lipke, P. N. and Conzelmann, A. (1995) *J Cell Biol* **130**, 1333-1344

29. Conzelmann, A. (2005) (Daum, G., ed.) pp. 133-159, Research Signpost, Trivandrum, Kerala, India

30. Watanabe, R., Funato, K., Venkataraman, K., Futerman, A. H. and Riezman, H. (2002) *J Biol Chem* **277**, 49538-49544

31. Ash, J., Dominguez, M., Bergeron, J. J., Thomas, D. Y. and Bourbonnais, Y. (1995) *J Biol Chem* **270**, 20847-20854

32. Tomishige, N., Noda, Y., Adachi, H., Shimoi, H. and Yoda, K. (2005) *Yeast* **22**, 141-155

33. Barz, W. P. and Walter, P. (1999) *Mol Biol Cell* **10**, 1043-1059

34. Reggiori, F., Canivenc-Gansel, E. and Conzelmann, A. (1997) *EMBO J* **16**, 3506-3518

35. Vossen, J. H., Muller, W. H., Lipke, P. N. and Klis, F. M. (1997) *J Bacteriol* **179**, 2202-2209

36. Sobering, A. K., Watanabe, R., Romeo, M. J., Yan, B. C., Specht, C. A., Orlean, P., Riezman, H. and Levin, D. E. (2004) *Cell* **117**, 637-648

37. Sipos, G., Reggiori, F., Vionnet, C. and Conzelmann, A. (1997) *EMBO J* **16**, 3494-3505

38. Fankhauser, C., Homans, S. W., Thomas-Oates, J. E., McConville, M. J., Desponds, C., Conzelmann, A. and Ferguson, M. A. (1993) *J Biol Chem* **268**, 26365-26374

39. Kapteyn, J. C., Ram, A. F., Groos, E. M., Kollar, R., Montijn, R. C., Van, D. E. H., Llobell, A., Cabib, E. and Klis, F. M. (1997) *J Bacteriol* **179**, 6279-6284

40. Ni, L. and Snyder, M. (2001) *Mol Biol Cell* **12**, 2147-2170

41. Leidich, S. D. and Orlean, P. (1996) *J Biol Chem* **271**, 27829-27837

42. Sipos, G., Puoti, A. and Conzelmann, A. (1994) *EMBO J* **13**, 2789-2796

43. Muniz, M., Nuoffer, C., Hauri, H. P. and Riezman, H. (2000) *J Cell Biol* **148**, 925-930

44. Fujita, M., Yoko-O, T., Okamoto, M. and Jigami, Y. (2004) *J Biol Chem* **279**, 51869-51879

45. Casamayor, A. and Snyder, M. (2002) *Curr Opin Microbiol* **5**, 179-186

Footnotes

Acknowledgements: We thank Howard Riezman, Taroh Kinoshita, Niahm Cawley, Yoshifumi Jigami, Dennis Voelker, Sabine Strahl and Peter Orlean for strains, plasmids and reagents. This work was supported by a grant from the Swiss National Science Foundation (31-67188.01).

Keywords not in title: Glycosylphosphatidylinositol; transamidase; saccharomyces; remodeling; ceramide; raft.

[1] **Abbreviations used:** CHX, cycloheximide; EtN-P, ethanolaminephosphate; GPI, glycosylphosphatidylinositol; IPC, inositolphosphorylceramide; KO, knock out; PE, phosphatidylethanolamine; PI, phosphatidylinositol; PI-PLC, PI-specific phospholipase C; TCA, trichloroacetic acid; ts, temperature sensitive; wt, wild type.

Figure legends

Figure 1: **Structure of the complete GPI precursor lipid CP2**. P = phosphate. The genes required for adding the EtN-P side chains and Man3 are indicated; yeast genes are in italics. Treatment of the lipid CP2 with hydrofluoric acid (HF), nitrous acid (HNO_2), and PI-PLC leads to hydrolysis at indicated sites.

Figure 2: ***T. brucei*** **Gpi10p can rescue viability and growth of yeast *mcd4*Δ cells**. **A**, the (*mcd4Δ/MCD4*) diploid strain was transformed with p425-*TbGPI10* carrying *TbGPI10* under the *MET17* promoter and was sporulated. One complete tetrad is shown. **B,** the genotype of strains T1 - T4 derived from the tetrad shown in panel A was evaluated by plating on methionine drop out and G418 plates. **C**, PCR analysis of the DNA of strains T1 - T4 and the parental *mcd4Δ/MCD4* diploid (P). The picture shows the homology regions of primers on the target DNA and the results of the PCR reactions done with various primer combinations as indicated. **D**, ten fold dilutions of T2 or T4 cells were plated on SDaaUA plates containing 2 mM ethanolamine (EtN), 50 mg/L inositol (Ins), 2 mM choline (C), 1 M sorbitol (Sor) alone or in combination. Plates were incubated at 37°C for 6 days.

Figure 3. ***mcd4*Δ*/TbGPI10*** **cells accumulate M4*. A,** Cells were labeled with [^{3}H]inositol (4 μCi/A_{600}) at 24°C (T1 - T4) or 37°C (*gpi7*Δ and *sec18 gpi8*) for 120 min. Desalted lipid extracts were analyzed by TLC using solvent $CHCl_3$:CH_3OH:H_2O (10:10:3) and fluorography. The same amount of radioactivity was spotted in each lane. Total incorporation into lipids was 24% in T1 and

T2, 17% in T3 and T4, 50% in *gpi7Δ* cells and 41% in *gpi8 sec18*. The small amounts of label comigrating with CP2 are due to incomplete desalting resulting in the presence of residual free [^{3}H]inositol (lane 1), which in this TLC run comigrated with CP2. **B**, lipid M4* of panel A was scraped off the plate, and the core glycan moiety was prepared using HF dephosphorylation. The N-acetylated glycan fragment was analyzed by paper chromatography and radioactivity was determined in 1 cm wide strips using scintillation counting. Certain standards (Std.) were run in parallel (M1-M4 = Man_x-GlcNAc-Inositol, x being 1, 3 or 4) while [^{14}C]inositol was mixed with the M4* test sample and its position is given by a vertical arrow (Ins). Free inositol contaminating the test sample may derive from partial degradation by HF. **C,** all cells were grown at 24°C and *gpi7Δ, mcd4^{ts}* and its corresponding *MCD4* wt strain were further incubated for two hours at 37°C. The cells were lysed and microsomes were prepared and incubated with UDP-[^{3}H]GlcNAc, GDP-Man, tunicamycin, nikkomycin, CoA and ATP for 1.5 h at the temperature used for the preculture. Lipids were extracted, desalted and analyzed by TLC as above. Lipids 4c and 031b are marked with open triangles and a circle, respectively.**D,** proteins remaining after lipid extraction in the experiment of panel A were analyzed by SDS-PAGE and fluorography.

Figure 4. **The *mcd4Δ/TbGPI10* cells contain reduced amounts of mature Gas1p**. **A**, T1 to T4 cells and the parental BY4742 cells were cultured in YPDUA at 30°C, protein extracts were prepared (19) and processed for Western blotting using antibodies against Gas1p and CPY and developed using the LI-COR system. The positions of mature (m), immature (i) and unprocessed precursors (p1, p2) are indicated. **B**, cells were grown in YPDUA at 30°C, media (M) and cell lysates (C) (solubilized with octyl-β-glucoside) were processed for Western blotting using anti-Gas1p antibodies and the ECL system.

Figure 5. **GPI-anchored Gas1p is not efficiently transported from the ER to the Golgi in *mcd4Δ/TbGPI10*. A,** 100 μg/ml cycloheximide (+CHX) or water (-CHX) were added to exponentially growing *MCD4/TbGPI10* (T1) or *mcd4Δ/TbGPI10* (T3) cells. After 20 min at 30 °C, the cells were lysed and proteins were solubilized with TX-114. After sedimenting at 16'000g for 5 min to remove insoluble material the supernatant was warmed to 37 °C and detergent (D) and aqueous (A) phases were separated and analyzed by Western blotting with anti-Gas1p antibody. The percentage of immature relative to total Gas1p, taking into account the sum of both phases, is indicated (%i). **B**, aliquots of the detergent phases from cells not incubated with CHX were diluted and incubated in the presence (+) or absence (-) of PI-PLC (PLC) to remove anchor lipids (Fig. 1). After incubation the samples were again separated into aqueous (A) and detergent (D) phases and were processed for immunoblotting as above. The percentage of Gas1p present in the aqueous (A) phase compared to the Gas1p in both (A + D) phases is indicated on separate lines for mature (%Am) and immature (%Ai) forms of Gas1p. **C**, the insoluble pellet (P) and the soluble supernatant (S) obtained during the initial 16'000g spin (see legend for panel A) were processed for immunoblotting as above. Material corresponding to equivalent amounts of cells was loaded. Blots of panels **A - C** were visualized using the LI-COR system. **D**, cells were labeled with [^{35}S]methionine/cysteine for 12 min and chased for 0 or 40 min. Gas1p was immunoprecipitated and analyzed by immunoprecipitation and autoradiography. *Sec18* cells were labeled at 37 °C, where they are unable to transport proteins out of the ER.

Figure 6. **Yap3p is not efficiently anchored in *mcd4Δ/TbGPI10*. A** and **B**, the lysates (**A**) and media (**B**) as used for Fig. 4B as well as lysates and media of *gpi1Δ* and *yap3Δ* prepared in parallel were analyzed for the presence of Yap3p by Western blotting. *Gpi1Δ* cells were grown at 24°C, incubated for 2 h at 37°C and lysed. An unspecific band (u) is pointed out. **C,** samples analyzed in Figs. 5A and 5B were also probed with anti-Yap3p antibodies and data were quantitated and expressed as in Fig. 5B.

Figure 7. **No ceramides are incorporated into the GPI anchors in *mcd4Δ/TbGPI10*.** BY4742 (wt) as well as T1 - T4 cells were labeled with [^{3}H]inositol, and the lipids were extracted with organic solvent; the protein pellets were further delipidated, GPI proteins were partially purified, digested with pronase and the thus generated GPI anchor peptides were subjected to HNO_2 treatment (Fig. 1) in order to release the labeled lipid moiety of the anchors. Lipid extracts of the cells (lanes 1 - 4) and anchor lipids (lanes 5 - 9) were separated by TLC using solvent $CHCl_3$:CH_3OH:0.25% aqueous KCl

(55:45:10 for lanes 1-3; 55:45:5 for lanes 4-9) and processed for fluorography. No lipids were seen when the HNO_2 treatment was omitted (lane 5), indicating that anchor peptides were not contaminated by free lipids. One of two experiments giving the same result is shown.

Figure 8. **Growth characteristics and hypersensitivities of *mcd4*Δ/*TbGPI10*. A,** serially 10 fold diluted T1 (wt) and T3 (mutant) cells were plated onto SDaaUA leu- met- drop out medium with or without 50 μg/ml calcofluor white and incubated for 4 days at 30°C. **B,** ten fold dilutions of exponentially growing cells were plated on YPDUA containing different inhibitors and incubated at 30°C for 3 days, except for plates containing Cu^{2+} which were incubated at 24°C. **C**, exponentially growing cells were streaked out on YPDUA plates preheated to 55°C. Thereupon the plates were first incubated for 45 min at 55°C, then for 3 days at 30°C.

Figure 9. ***mcd4*Δ/*TbGPI10* cells have a bud site selection defect. A** and **B**, cells were kept in continuous culture at 30 °C during 10 generations and stained with calcofluor white and photographed. The prevalent types of scar patterns are shown. The *mcd4*^{ts} cells were grown at semipermissive temperatures (32 or 34°C). The *gpi1* mutant grows at 30°C but is unable to grow at 32°C.

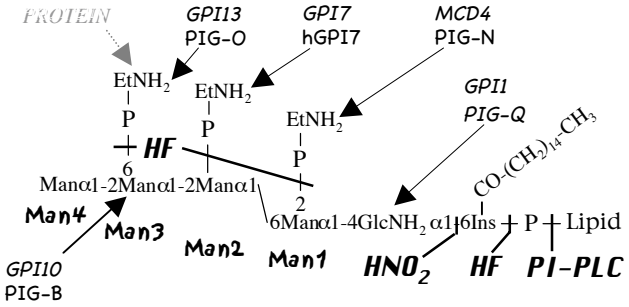

Figure 1

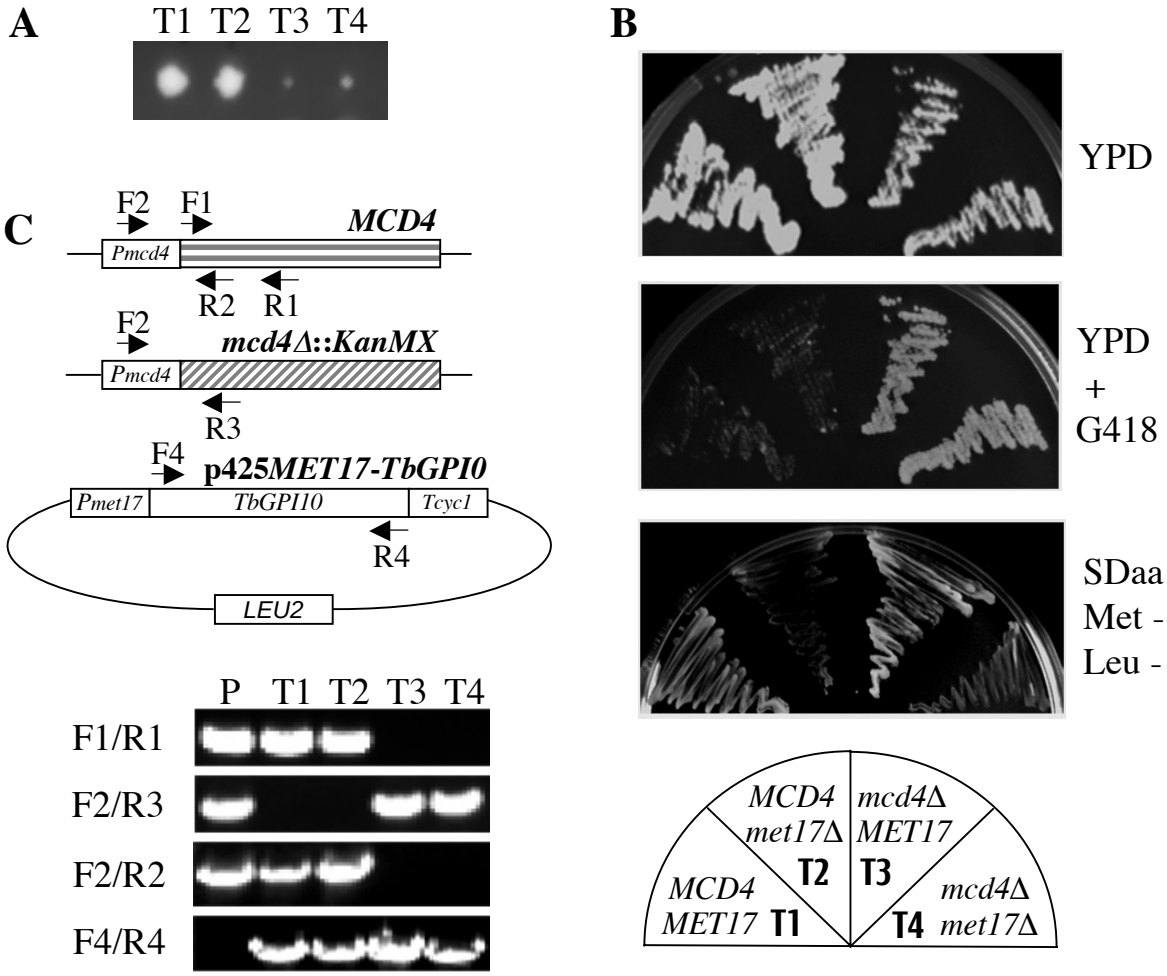

Figure 2

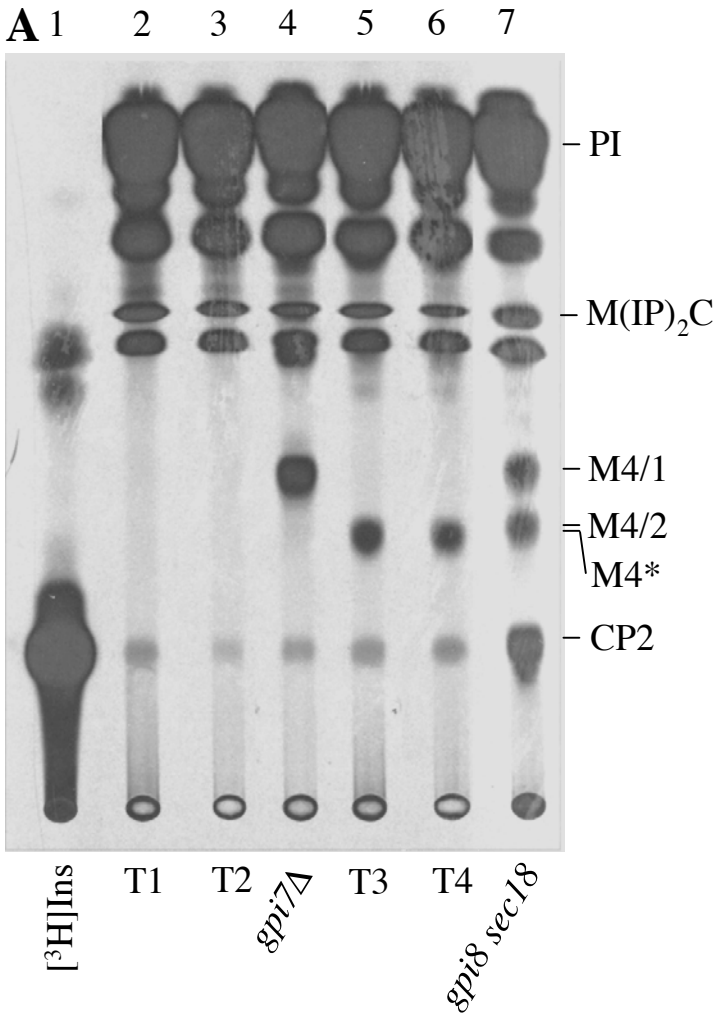

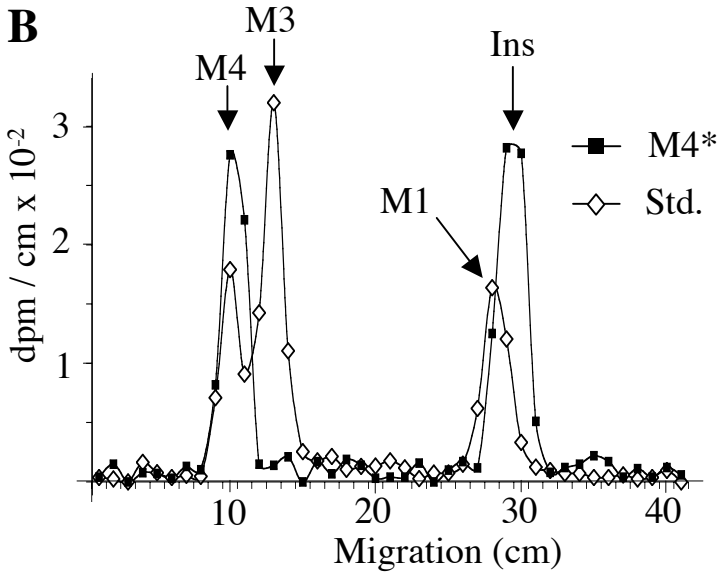

Figure 3A, B

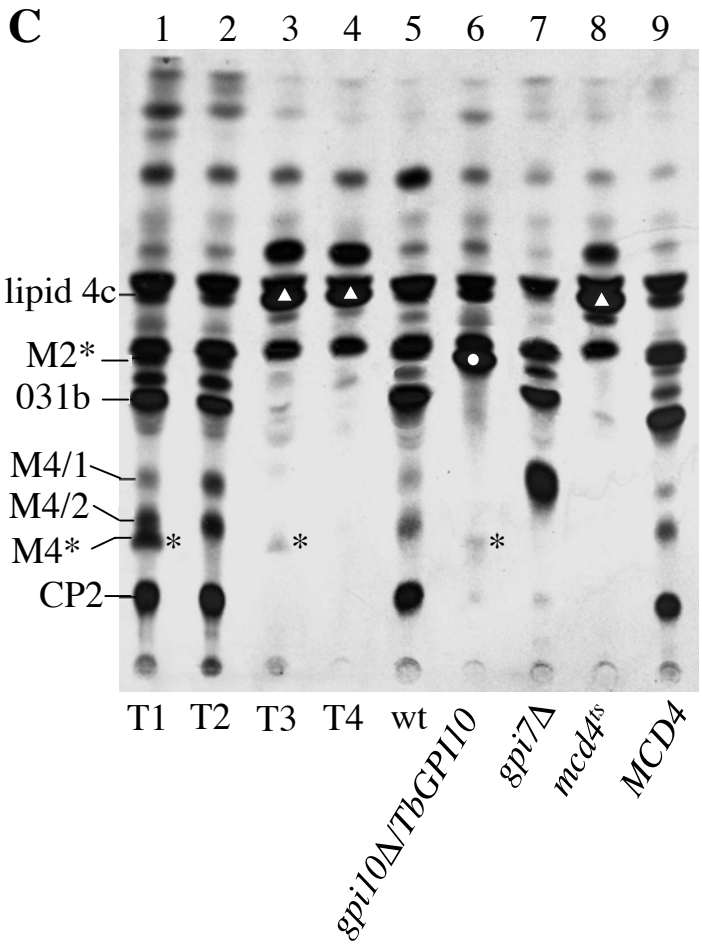

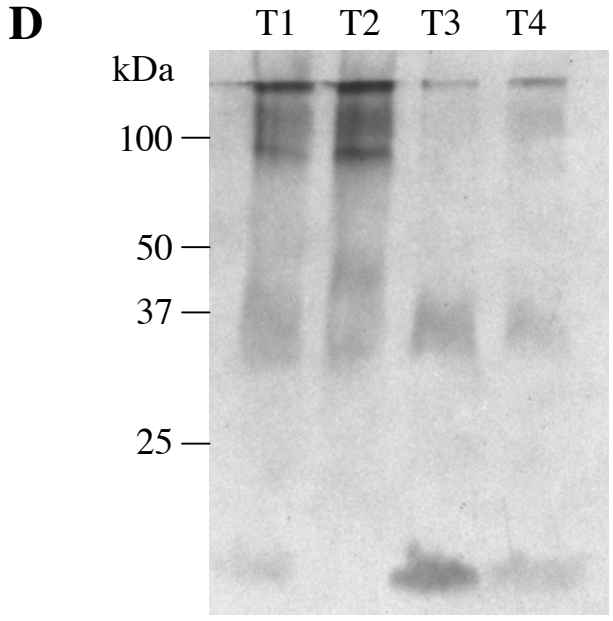

Figure 3C, D

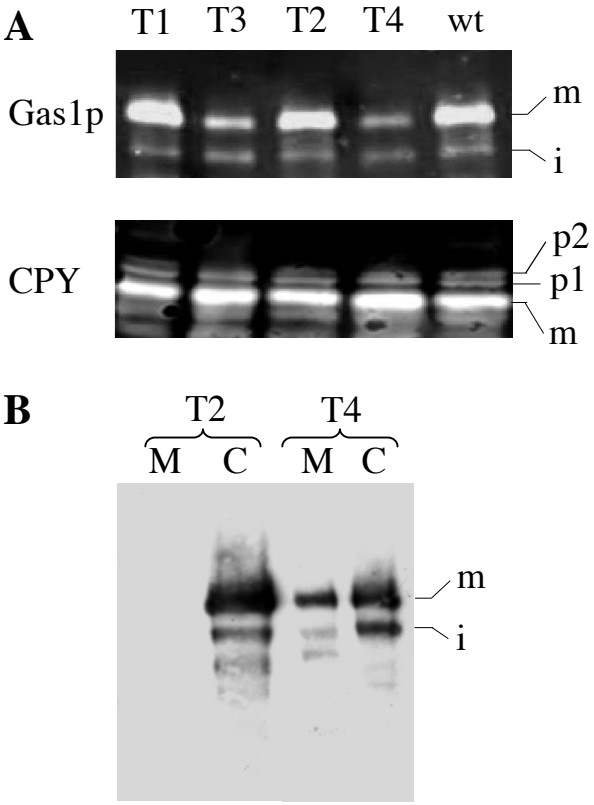

Figure 4

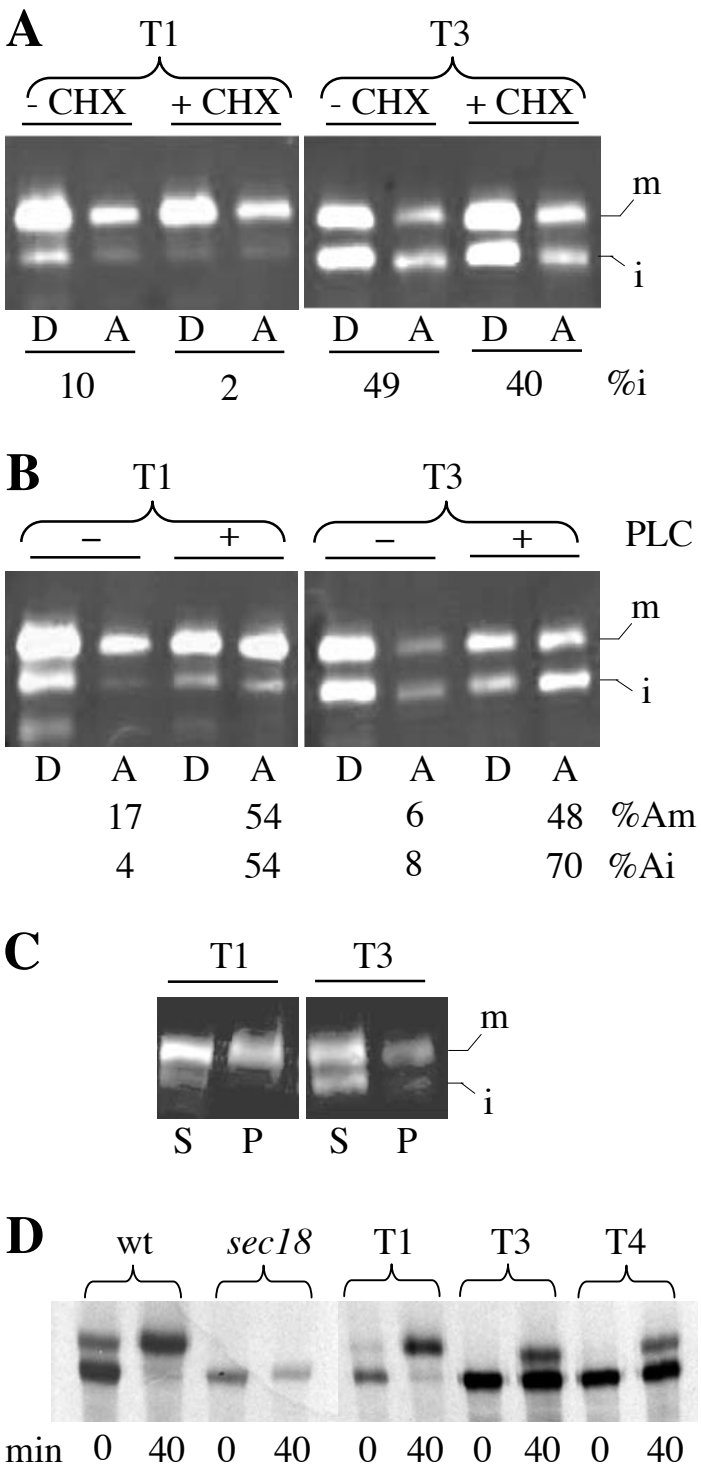

Figure 5

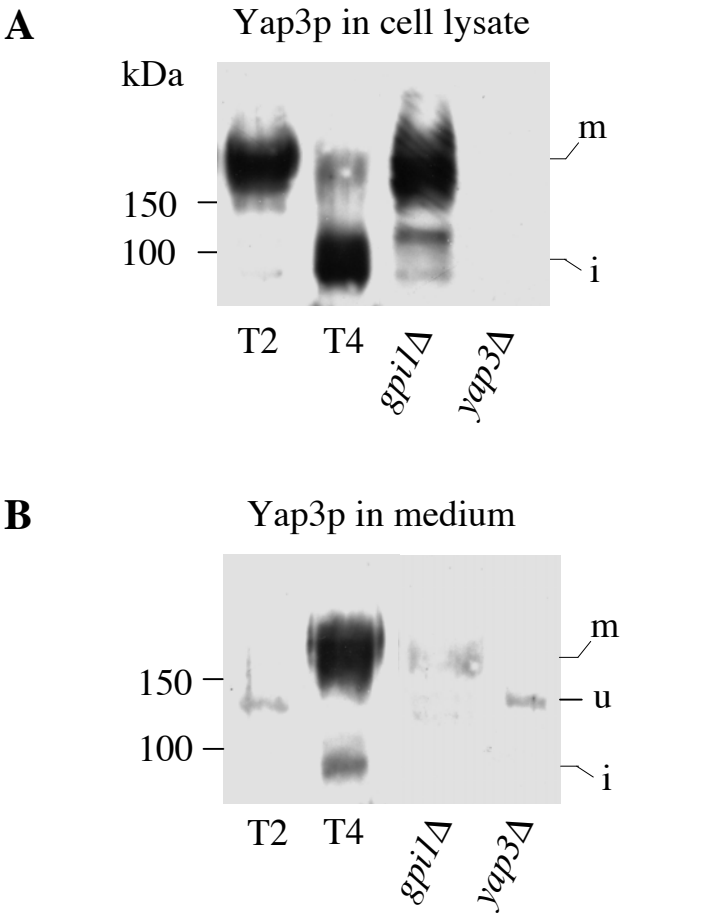

Figure 6

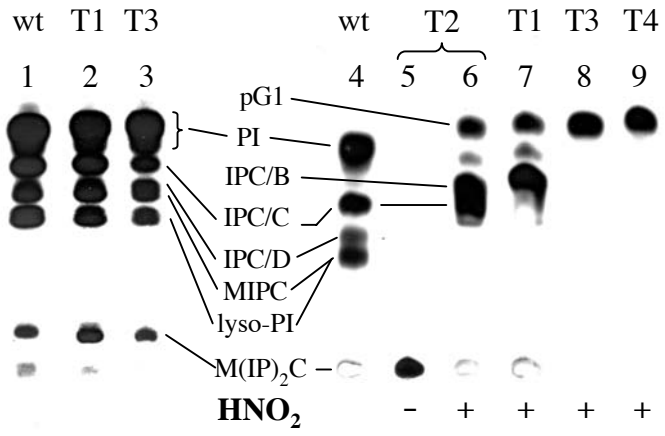

Figure 7

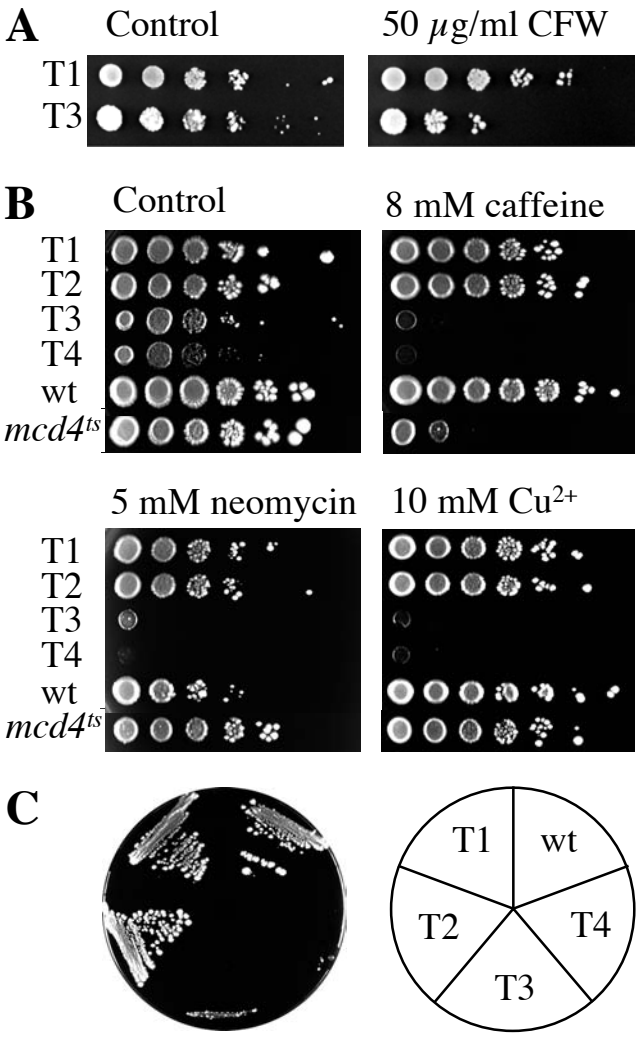

Figure 8

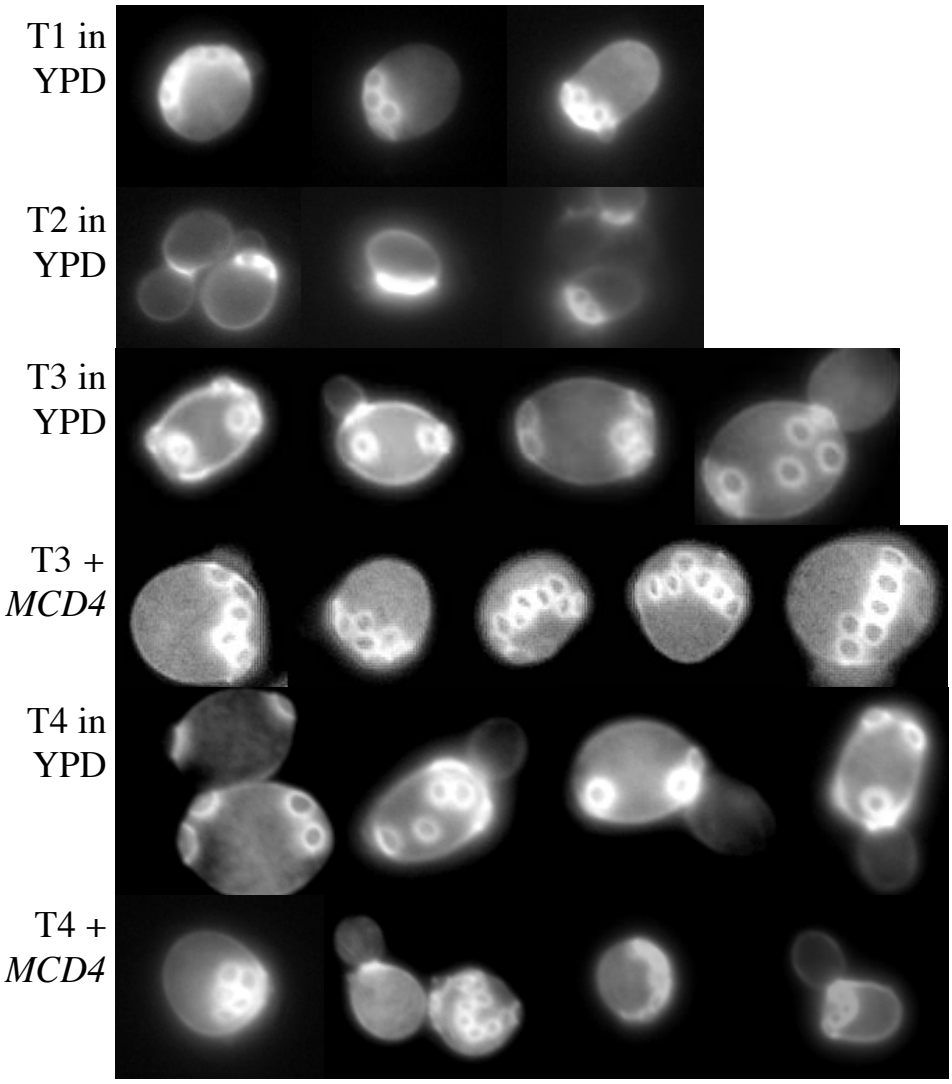

Figure 9A

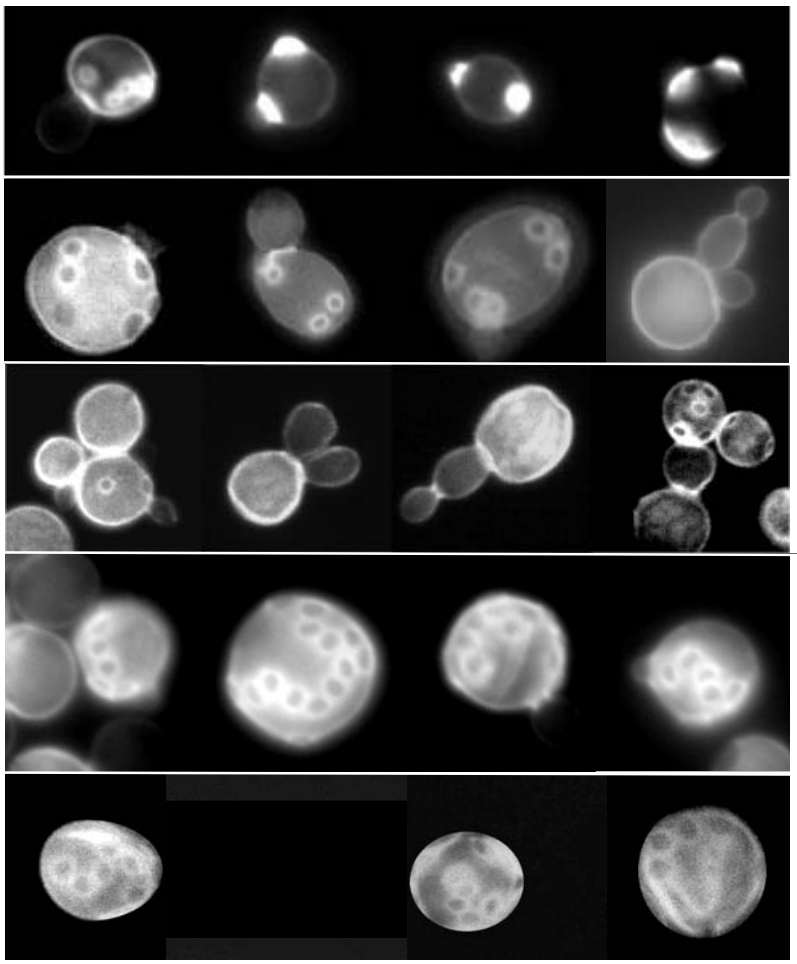

Figure 9B